CFSRC COLLOQUIUM

Proceedings of the Cold-Formed Steel Research Consortium Colloquium
17-19 October, 2022 (cfsrc.org)

Numerical study on residual stresses in press-braked advanced high-strength cold-formed steel angles by finite element simulation

Yu Xia[1], Zhanjie Li[2], Hannah B. Blum[3]

Abstract

Cold-formed steel is widely used in structural framing for its beneficial high strength-to-weight ratio, recyclability, and for convenient transportation and construction. The rapid advancement of metallurgy during the past two decades has resulted in a new family of steel known as advanced high-strength steel (AHSS) that has a unique microstructure which enables unprecedented combinations of strength and ductility. The material properties and behavior of the AHSS structural members must be quantified to bring AHSS to the construction industry. The cold-forming process, such as press-braking, induces residual stresses which affect the strength and stability behavior of the structural members. Existing numerical studies quantified the residual stress of conventional cold-formed steel, but studies of residual stresses in high-strength cold-formed steel are limited. This paper develops computational models to simulate the press-brake process of cold-formed AHSS sections and investigates their residual stress distribution through the simulation. The results are validated with recently conducted experimental studies. Numerical modeling of the press-braking process on AHSS angles by the finite element method was conducted. The model incorporated the residual stresses induced by coiling and uncoiling before the press-braking operation was performed. Lipped angles were studied where the angles were press-braked from a 1.8-mm thick dual-phase steel sheet with a nominal yield strength of 580 MPa and a nominal ultimate strength of 980 MPa. Two different inner corner radii, 1.98-mm and 3.57-mm (5/64-inch and 9/64-inch), were investigated. Stresses at the cross-section corners, legs, and lips on both inner and outer surfaces along the sheet coiling direction were extracted from the analysis results. The stress data from the simulation was validated with its counterparts from a series of experimental measurements using the sectioning method, which are presented in a companion paper.

1. Introduction

Cold-formed steel (CFS) open-sections are widely used in structural framing for its beneficial high strength-to-weight ratio, recyclability, and convenient transportation and construction. Due to the rapid advancement of material science during the past two decades, new grades of steel, known as advanced high-strength steel (AHSS), have been developed and used in the automobile industry. To bring AHSS to the construction industry, the material properties and behavior of the structural sections composed of this material must be quantified. This includes the residual stresses induced in the structural members as a result of the cold-forming process. The distribution and magnitude of residual stresses affect the strength and stability behavior of the CFS members.

In existing studies, many researchers experimentally investigated the residual stress distribution by sectioning method [1]–[3] for both press-braked and roll-formed conventional CFS open-sections [4]–[12]. Using the sectioning method to measure the residual stress is straightforward and the results are relatively reliable. However, the sectioning method is a destructive method with considerably high time, labor, and equipment costs. Therefore, conducting a large number of sectioning tests is challenging and costly. Additionally, for the CFS open-sections with thin-walled geometry, only the residual stresses at section surfaces can be measured, but the residual stresses through the steel sheet thickness direction cannot be directly measured because it is difficult to install the strain gauges at non-surface locations through the sheet thickness. Furthermore, from existing studies on residual stress distribution for CFS sections [8], [13]–[17], the maximum residual stresses are frequently observed at non-surface locations throughout the steel sheet thickness and the residual stress distributions along the steel thickness direction vary based on the steel material property, forming method, and geometry (e.g., cross-section shape and sheet thickness). Additionally, available residual stress data for cold-formed high-strength steel sections are highly limited.

[1]Graduate Research Assistant, Department of Civil & Environmental Engineering, University of Wisconsin-Madison, yxia44@wisc.edu

[2]Associate Professor, Engineering Department, State University of New York Polytechnic Institute zhanjie.li@sunypoly.edu

[3]Assistant Professor, Department of Civil & Environmental Engineering, University of Wisconsin-Madison, hannah.blum@wisc.edu

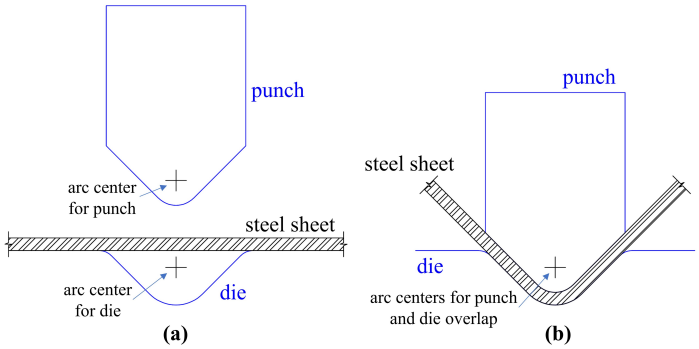

Figure 1: A sketch map for the positions of punch, die, and steel sheet when the press braking process (a) starts and (b) finishes.

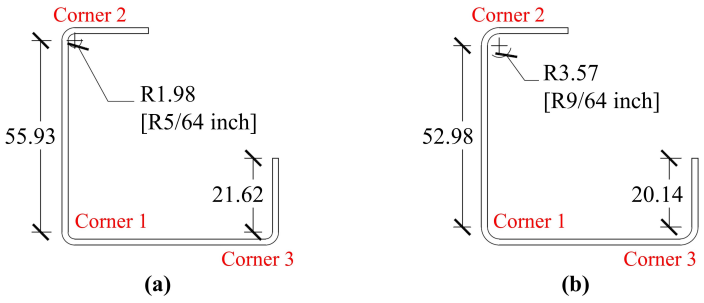

Figure 2: Design geometry for (a) small corner radius cross-section and (b) large corner radius cross-section.

In this paper, a finite element model is developed to simulate the section forming process of the press-braked DP-580 lipped angle sections with two different corner radii. The model is validated by comparing the results between the companion experimental study [18] and this numerical study. A step-wise simulation procedure is proposed to accurately simulate the successive forming of the multiple corners of the lipped angles. In addition, the effect on the member residual stress distribution from the geometry of the die is investigated. Finally, in addition to the residual stresses at steel sheet surfaces, the residual stress distribution through sheet thickness is extracted from the simulation results and discussed.

2. Simulation setup

Press-braking is a popular manufacturing method for steel member forming, particularly those steel sheets with relatively low thicknesses. The steel sheet is placed on the die and the punch moves vertically downwards to a predefined location to bend the steel sheet along the steel section longitudinal direction until the forming of a corner for the steel section, where a representative diagram is shown in Fig. 1. Subsequently, the punch moves upwards to its original position, and as the force between the steel sheet and the punch is relieved a spring-back of the steel sheet occurs. The residual stress distribution in the steel section is affected by the spring-back effect, therefore, to accurately model the residual stress distribution due to press-braking, both the press-braking and spring-back processes must be simulated.

The finite element software Abaqus [19] was used to simulate the forming process of the press-braked DP-580 lipped angle sections [18] by constructing 2D plane stress analyses. The forming process of each corner consisted of two steps, which including press-braking and spring-back. Three corners for each angle section were formed sequentially as labeled by the red annotations in Fig. 2. Two different inner corner radii (1.98-mm and 3.57-mm, or 5/64-inch and 9/64-inch) were investigated and the design geometry for the cross-sections is shown in Fig. 2. The section with the larger corner radius was labelled as RL (radius-large) and the section with the smaller corner radius was labelled as RS (radius-small).

The residual stresses for the press-braked steel sections result from the CFS sheet forming (i.e., coiling, uncoiling, and flattening processes) and CFS section forming (i.e., press-braking and spring-back processes). Therefore, before the simulation of the press-braking and spring-back processes, it was essential to accurately predefine the residual stress generated during the CFS sheet forming, where the residual stress distribution model proposed by Moen and Schafer [20] was adopted. When adopting the model, the model parameter r_x (coil radius) was back-calculated using Eq. 1 by assuming the residual stresses generated during the sheet forming at the outer and inner surfaces of any cross-section location equalled the average of all measured residual stresses at the outer and inner surfaces of measured locations on flat regions of the legs (i.e., the measuring locations (f), (g), (h), and (i) in the experimental study [18] as shown in Fig. 3):

$$\sigma_z^{coil}+\sigma_z^{uncoil}+\sigma_z^{flatten} = \frac{1}{2n}\cdot\sum_{i=1}^{n}(\mid \sigma_i^{leg,in} \mid + \mid \sigma_i^{leg,out} \mid) \quad (1)$$

where σ_z^{coil}, σ_z^{uncoil}, and $\sigma_z^{flatten}$ are the longitudinal residual stresses generated during coiling, uncoiling, and flattening processes respectively and they can be expressed in the form of r_x as described in [20], $\sigma_i^{leg,in}$ and $\sigma_i^{leg,out}$ are the longitudinal residual stresses at the inner and outer surfaces of the flat leg regions measured in the experimental study [18], n is the number of the measuring locations on the flat leg regions for the experimental study [18].

For the direction of the predefined residual stresses generated during the steel sheet forming, it was reasonable to assume that the direction of the residual stress generated during coiling, uncoiling, and flattening in the model was consistent with that of the test result [18] at the flat region of the

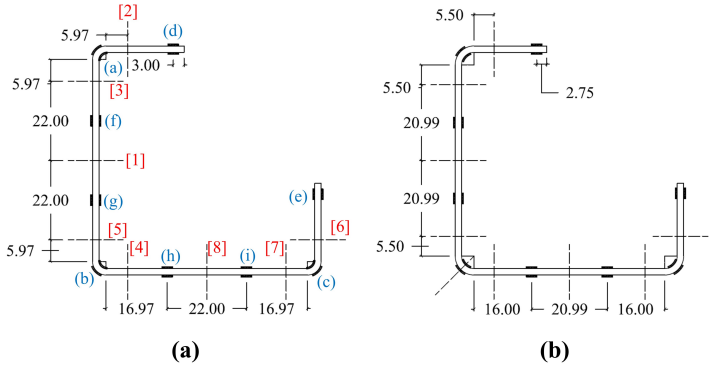

Figure 3: Measuring locations of strain gauges and sectioning locations in the experimental study [18] for (a) small corner radius cross-section and (b) large corner radius cross-section. Blue letters are the indices for measuring locations. Dashed lines are the sectioning locations. Red numbers are the sectioning sequence.

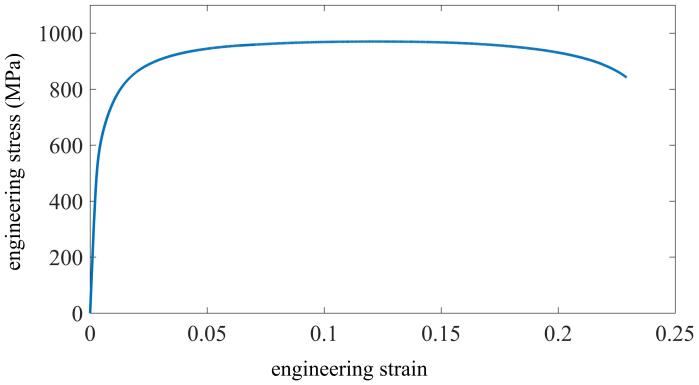

Figure 4: Engineering stress-strain relationship for DP-580 sheet generated using data from tensile coupon test [21]

legs, where the stresses on the inner surface were negative and on the outer surfaces were positive. By using the calculated r_x and the speculative residual stress direction, the residual stress distribution generated during the CFS sheet forming was obtained, which was input into the model as predefined stress.

The punch and die of the Accurpress Hydraulic CNC Press Brake Model 713012 as used for the forming of the lipped angle sections in [18] were designed as 2D discrete rigid parts and therefore were meshed using discrete rigid elements, because the deformation of the punch and the die is negligible compared with the deformation of the the steel sheet. The geometry of the punch and the die were initially designed to perfectly fit the desired steel corner deformation, where the arc radius of the punch equaled the inner corner radius of the steel cross-section and the arc radius of the die equaled the outer corner radius of the steel cross-section. The arc centers of the punch and the die coincide when the press-braking process completes as illustrated in Fig. 1.

The steel sheet was 1.8 mm thick. It was designed as a 2D deformable part and was meshed using CPE4R element (four-node plane strain element), which is suitable for steel sheets with thin-walled geometry subjected to large strains. The width of the steel sheet equaled the perimeter of the cross-section centerline, which was 172.7-mm for RL section and 171.9-mm for RS section. A series of preliminary simulation was conducted to determine the appropriate element size for the steel sheet. It was found that when the number of elements through the sheet thickness direction was 20 or above, the longitudinal stress did not vary noticeably. Considering a balance between simulation accuracy and computation demand, the element size was selected as 0.09-mm, which corresponded to 20 elements through the 1.8-mm thickness.

For the material definition of the steel sheet, an engineering stress-strain relationship was generated as shown in Fig. 4 using the two-stage plus linear model as proposed in [21], where the model parameters were selected as the averages of the experimental stress-strain data for DP-580 tensile coupons cut along sheet longitudinal direction [21].

The generated engineering stress-strain curve was converted to true stress-strain curve by Eq. 2 and 3, where σ_t and ε_t are the true stress and strain, σ_e and ε_e are the engineering stress and strain. In Abaqus, the material property is defined by the true post-yield stress and true plastic strain, which were converted from the true stress-strain curve.

$$\sigma_t = \sigma_e \times (1 + \varepsilon_e) \tag{2}$$

$$\varepsilon_t = \ln(1 + \varepsilon_e) \tag{3}$$

To simulate the actual forming process, a contact was built between the punch head and the cross-section inner surface during the press-braking process, while this contact was released during the spring-back process. Another contact was defined between the die and the outer surface of the steel sheet for both press-braking and spring-back processes since the steel sheet was placed on the die for the entire process.

For the boundary conditions, the die was fully fixed during both the press-braking and spring-back processes, the punch was fixed in all directions except the loading direction, and the steel sheet was not restrained in any direction. A displacement-control loading was applied for the punch along a local direction which was perpendicular to the sheet at the designated corner. The displacement magnitude was set from the arc center of the punch to the arc center of the die until the two arc centers overlapped. Once finished, the

exact displacement was set back to zero during the spring-back process to simulate the lift-up of the punch after the press-braking process.

A step-wise dynamic implicit analysis strategy was developed and adopted in the simulation. Each step represented the press-braking and spring-back processes for each cross-section corner. For the press-braking and spring-back processes in each step (i.e., the forming of each corner), the initial and minimum increment sizes for both processes were 10^{-4} and 10^{-15} respectively. Three steps were conducted for each lipped angle section. For the second and the third steps, the deformed cross-section geometry and the stresses and strains in each element resulting from the previous step(s) were required as input. Therefore, the deformed section geometry was imported as a new part and the stress state was imported as a predefined initial state from the output database from the previous step. For each step, the punch head was placed perpendicular to the inner surface of the desired corner location and the horizontal support of the die was placed at the corresponding outer surface of the steel sheet. The placement of the steel sheet, the punch, and the die for each step in the model is shown in Fig. 5.

Additionally, it was found that the residual stress distribution and magnitudes were significantly affected by the arc radius of the die. When the die perfectly fit the design dimension (the die radius for this situation was labeled as R_0), the outer surface of the steel sheet experienced full direct contact with the die due to the sheet deformation along the sheet thickness direction. When a sharp die (i.e., arc radius of the die equals zero) was adopted, this full contact could be avoided. The longitudinal residual stress distributions for members press-braked with a fully rounded die and a sharp die are shown in Fig. 6. Considering the inevitable uncertainties during the steel cross-section forming, plus the unknown dimension for the die being used, the residual stress magnitude and distribution by using different arc radii of the dies between 0 and R_0 were investigated. Besides the arc radii of the dies, all other procedures and setups for the simulation were identical.

3. Simulation results

The stresses along the direction perpendicular to the plane (i.e., S33 of the output database) were extracted. The width of the strain gauge used in the experimental study [18] was 1.5-mm, which corresponds to approximately 17 elements. The average stresses of S33 for the center 17 elements at each corner position for both outer and inner surfaces were calculated and used for comparison with test data.

By varying the arc radius of the die between 0 and R_0, certain radii were selected which exhibited reasonable tolerances between the results of experiments and simulation. The selected arc radii of the dies were 3.634-mm for RS sections and 4.72-mm for RL sections respectively. The comparison for the longitudinal residual stresses on the inner and outer surfaces at the measuring locations between the test data and the simulation results using three different arc radii of the dies ($r = R_0$, $r = 0$, and the selected radius) are shown in Fig. 7 for RS sections and Fig. 8 for RL sections respectively. For the "position" axes, 0.9-mm represents the inner surface and -0.9-mm represents the outer surface.

The comparison shows the selected radius simulation cases have minimal differences from the corresponding experiment data at the corners, where the residual stresses are more pronounced. The residual stresses at the flat region have relatively large percentage differences, while the absolute differences are small, which lead to negligible influence on steel member strength.

Fig. 7 and 8 also illustrate the through-thickness residual stresses captured from the simulation. For both RS sections and RL sections at corners, the maximum stresses are observed at around a quarter of the thickness away from the inner surface and the maximum stresses are in compression as high as 700 MPa. Additionally, the stresses are observed to vary drastically between the inner surface and the centerline of the steel sheet.

For the measuring locations on the flat regions, the residual stress distribution is similar to the predefined stress state generated using the model developed in [20], where the stress magnitude is relatively low. Besides, at those flat regions, the residual stress distribution through thickness is generally symmetric to the steel sheet centerline, and the residual stress for the non-surface elements are close to zero. This indicates steel member forming (i.e., press-braking and spring-back processes) does not significantly affect the residual stress distribution for the flat regions.

4. Conclusions

A finite element model was developed to simulate the section forming of cold-formed DP-580 press-braked lipped angle sections with two different radii. The model was validated by the corresponding experimental results from surface residual stress measurements using sectioning method. A step-wise simulation strategy was proposed to simulate the forming of each corner of the lipped angles. From the simulation results, it was found that the geometry of the die significantly affected the residual stress distribution of the steel sections, and certain arc radii for the dies were recommended, which illustrated good agreements with the test data. In addition, by adopting the validated model, the residual stress distribution through steel sheet thickness direction was illustrated, where the maximum residual stresses of around 700 MPa in compression at the corners were observed and drastic vari-

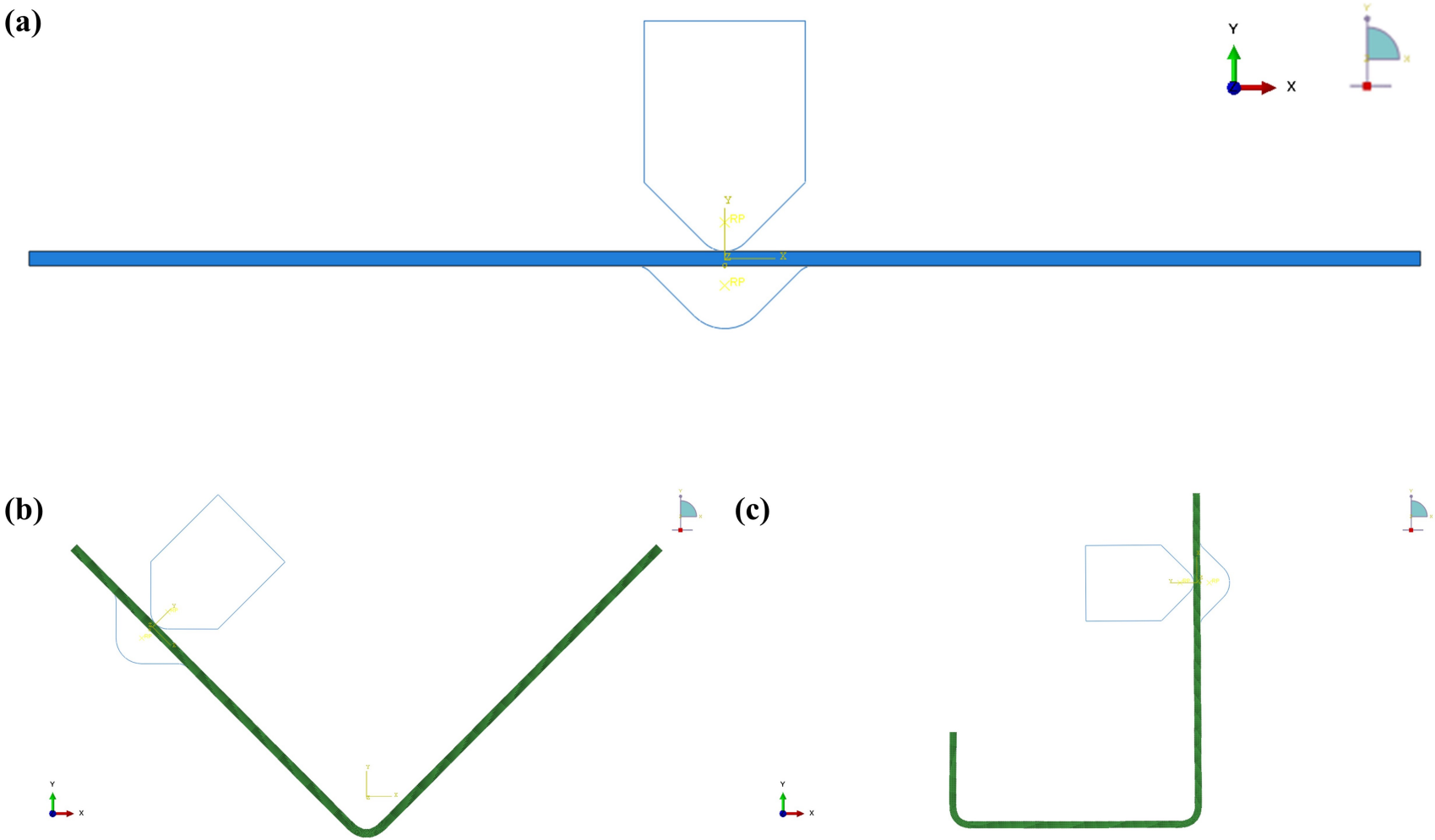

Figure 5: The placement of the steel section, punch, and the die for (a) the first step, (b) the second step, and (c) the third step.

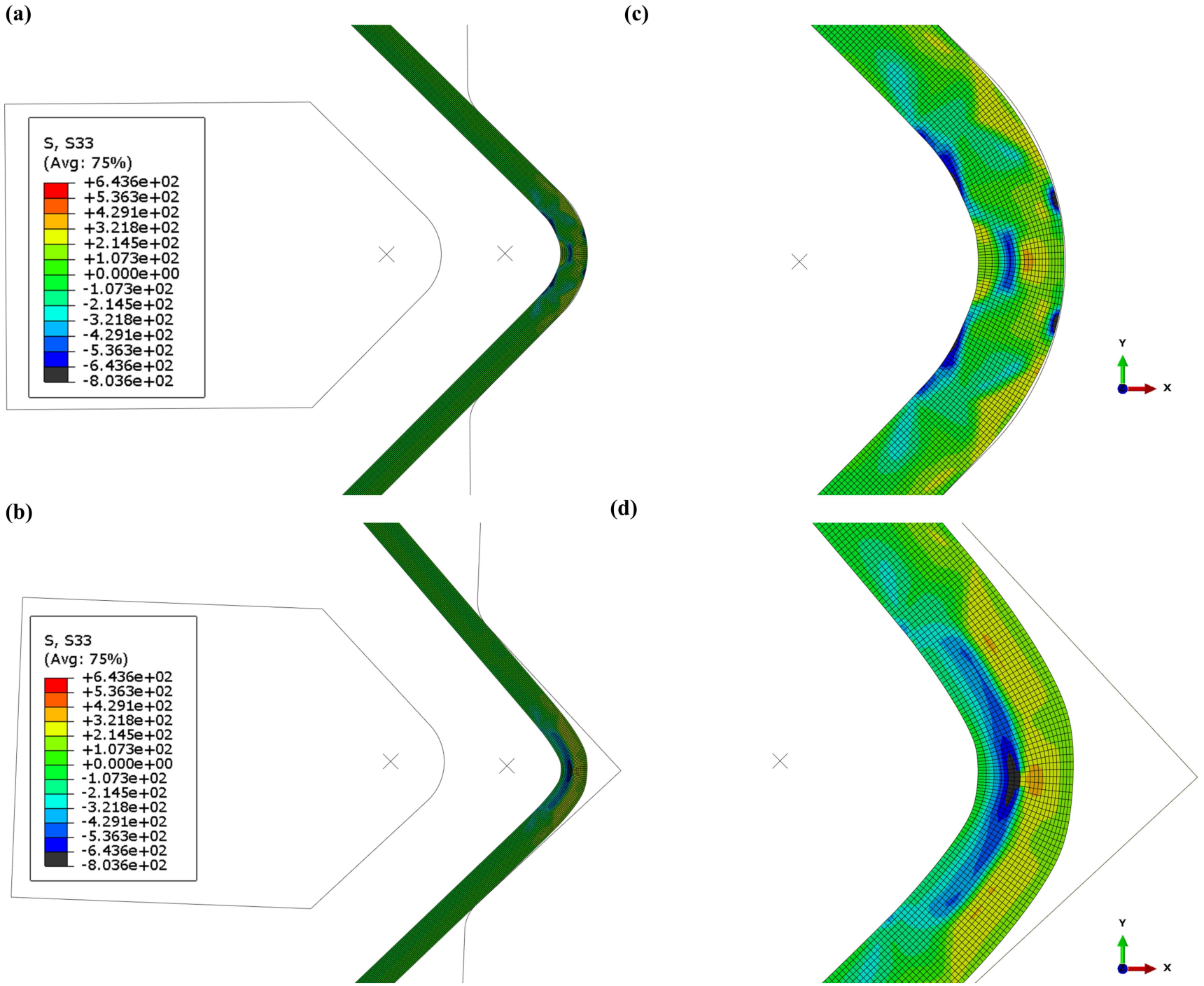

Figure 6: (a) and (b): deformation of the angle member after press-braking and spring-back processes using rounded and shape die respectively. (c) and (d): a close look of (a) and (b) illustrating the longitudinal residual stress distribution through member thickness at angle corners.

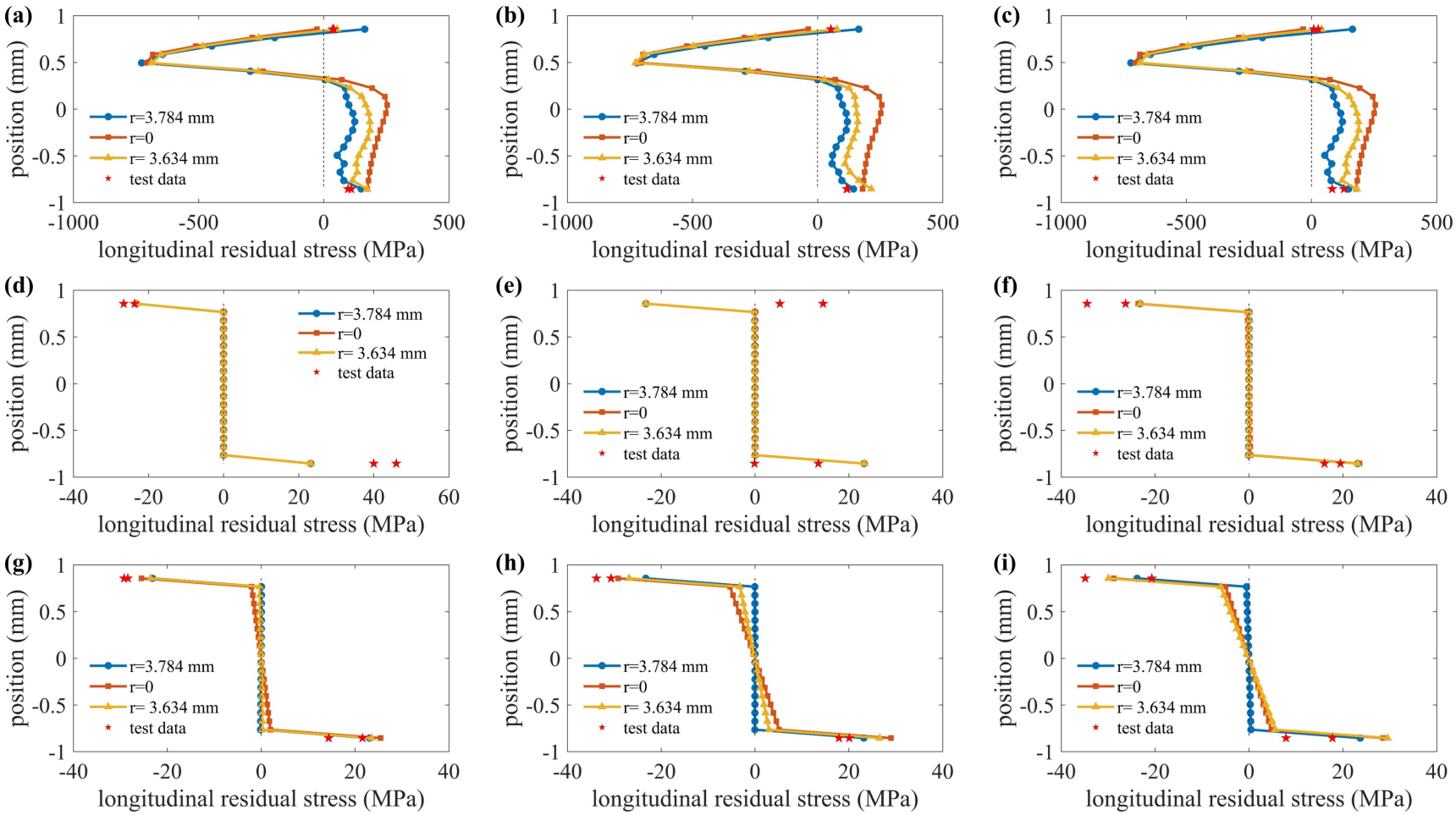

Figure 7: Comparison between the test results and the simulation results with three different die shapes for RS sections. The subplot indices (a) to (i) correspond to the same measuring locations shown in Fig 3.

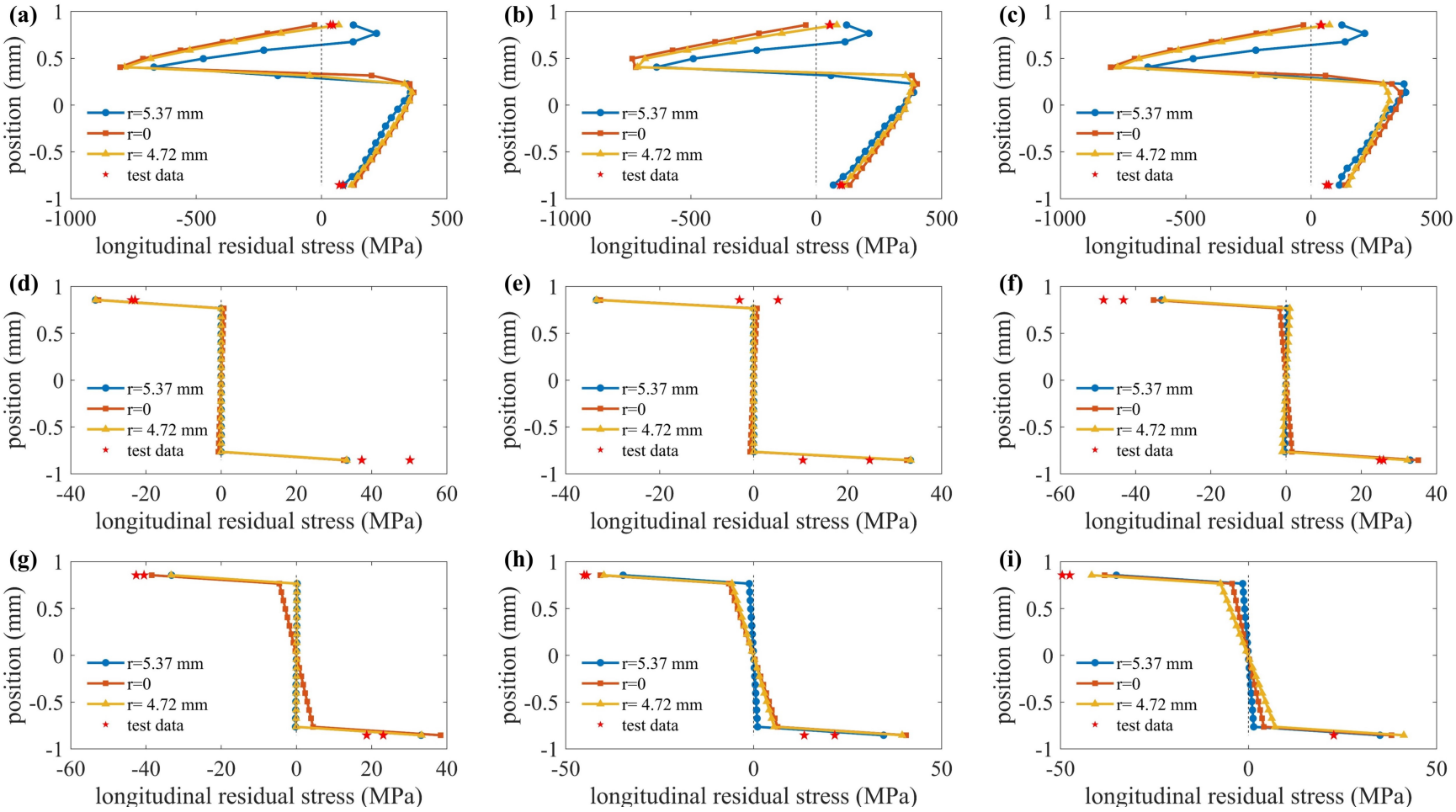

Figure 8: Comparison between the test results and the simulation results with three different die shapes for RL sections. The subplot indices (a) to (i) correspond to the same measuring locations shown in Fig 3.

ations of the through-thickness residual stresses at the corners were noticed.

Acknowledgments

The authors would like to thank Prof. Benjamin Schafer at Department of Civil and Systems Engineering, Johns Hopkins University for his suggestions on the technical issue resolving of this numerical study.

References

[1] N. Kalakoutsky, *The study of internal stresses in cast iron and steel*, 1888.

[2] N. Tebedge, G. Alpsten, and L. Tall, "Residual-stress measurement by the sectioning method," *Experimental Mechanics*, vol. 13, no. 2, pp. 88–96, 1973.

[3] T. Pekoz, R. Bjorhovde, S. Errera, B. Johnston, D. Sherman, and L. Tall, "Determination of residual stresses in structural shapes," *Experimental Techniques*, vol. 5, no. 3, pp. 4–7, 1981.

[4] L. Ingvarsson, "Cold-forming residual stresses effect on buckling," 1975, pp. 85–119.

[5] D. T. Dat and T. Peköz, "The strength of cold-formed steel columns," Cornell University, 1980. [Online]. Available: https://scholarsmine.mst.edu/ccfss-library/110.

[6] J. Coestee, G. Van den Berg, and P. Van der Merwe, "The effect of work hardening and residual stresses due to cold-working of forming on the strength of cold-formed stainless steel lipped channel sections," in *10th International Specialty Conference on Cold-Formed Steel Structures, St. Louis, Missouri*, 1990.

[7] C. C. Weng and T. Peköz, "Residual-stresses in cold-formed steel members," *Journal of Structural Engineering-ASCE*, vol. 116, no. 6, pp. 1611–1625, 1990.

[8] C. Weng, R. White, *et al.*, "Residual stresses in cold-bent thick steel plates," *Journal of Structural Engineering-ASCE*, vol. 116, no. 1, pp. 24–39, 1990.

[9] E. de M. Batista and F. Rodrigues, "Residual stress measurements on cold-formed profiles," *Experimental Techniques*, vol. 16, pp. 25–29, 5 1992. DOI: 10.1111/j.1747-1567.1992.tb00702.x.

[10] B. Young and K. Rasmussen, *Compression tests of fixed-ended and pin-ended cold-formed lipped channels*, Sep. 1995.

[11] N. Abdel-Rahman and K. Sivakumaran, "Material properties models for analysis of cold-formed steel members," *Journal of Structural Engineering*, vol. 123, no. 9, pp. 1135–1143, 1997.

[12] E. Ellobody and B. Young, "Behavior of cold-formed steel plain angle columns," *Journal of Structural Engineering*, vol. 131, no. 3, pp. 457–466, 2005.

[13] W. Quach, J. Teng, and K. F. Chung, "Finite element predictions of residual stresses in press-braked thin-walled steel sections," *Engineering structures*, vol. 28, no. 11, pp. 1609–1619, 2006.

[14] W. Quach, J. Teng, and K. F. Chung, "Residual stresses in press-braked stainless steel sections, ii: Press-braking operations," *Journal of Constructional Steel Research*, vol. 65, no. 8-9, pp. 1816–1826, 2009.

[15] H. Amouzegar, B. Schafer, and M. Tootkaboni, "An incremental numerical method for calculation of residual stresses and strains in cold-formed steel members," *Thin-Walled Structures*, vol. 106, pp. 61–74, 2016.

[16] Y. Sun, V. Luzin, S. Khan, *et al.*, "Understanding of residual stresses in chain-die-formed dual-phase (dp) metallic components: Predictive modelling and experimental validation," *The International Journal of Advanced Manufacturing Technology*, vol. 103, no. 9, pp. 3337–3360, 2019.

[17] A. Mutafi, N. Yidris, J. Loughlan, R. Zahari, and M. Ishak, "Investigation into the distribution of residual stresses in pressed-braked thin-walled steel lipped channel sections using the 3d-fem technique," *Thin-Walled Structures*, vol. 135, pp. 437–445, 2019.

[18] Y. Xia and H. B. Blum, "Experimental study on residual stresses in press-braked advanced high-strength cold-formed steel lipped angles by sectioning method," in *Proceedings of the Cold-Formed Steel Research Consortium Colloquium*, 2022.

[19] Abaqus, *version 6.16*. Dassault Systèmes Simulia Corp, 2016.

[20] C. D. Moen, T. Igusa, and B. W. Schafer, "Prediction of residual stresses and strains in cold-formed steel members," *Thin-walled structures*, vol. 46, no. 11, pp. 1274–1289, 2008.

[21] Y. Xia, C. Ding, Z. Li, B. W. Schafer, and H. B. Blum, "Numerical modeling of stress-strain relationships for advanced high strength steels," *Journal of Constructional Steel Research*, vol. 182, p. 106 687, Jul. 2021, ISSN: 0143974X. DOI: 10.1016/j.jcsr.2021.106687.